ELSEVIER

Chemical Engineering Journal 86 (2002) 309–317

Chemical Engineering Journal

www.elsevier.com/locate/cej

Influence of fractal pore structure in Claus catalyst performance

Rafael Larraz*

Chemical Engineering Department, University of La Laguna. Avda. Astrofísico Francisco Sánchez s/n, 38200 La Laguna, Tenerife, Canary Islands, Spain

Received 7 December 2000; accepted 12 June 2001

Abstract

The Claus process is an efficient way of removing H_2S from acid gas streams and it has been widely practised in industries such as natural gas processing, oil refining and metal smelting. Catalytic stage plays a paramount role in Claus units performance. Different samples of Claus reaction alumina catalyst were characterised by the fractal dimension parameter employing nitrogen adsorption porosimetry. The influence of such a dimension over Claus reactor performance was studied employing a reactor model. Significant differences between fractal and smooth catalysts performance were found as well as implications in reactor design. Deactivated catalyst samples were also characterised and its behaviour as Claus catalyst shows influence of the fractal dimension value. Fractal dimension appears as a useful parameter to the Claus catalyst selection procedure.

Keywords: Claus catalyst; Fractal dimension; Thiele modulus

1. Introduction

The Claus process is an efficient way of removing H_2S from acid gas streams and it has been widely practised in industries such as natural gas processing, oil refining and metal smelting. Increasingly strict pollution control regulations require maximum sulphur recovery from the Claus unit in order to minimise sulphur-containing effluent. Claus reaction consists of hydrogen sulphide and sulphur dioxide reaction in vapour phase to produce sulphur and water.

$$3H_2S + 1.5O_2 \Rightarrow 2H_2S + SO_2 + H_2O$$

$$2H_2S + SO_2 \Leftrightarrow (3/x)S_x + 2H_2O$$

Here S_x is the sulphur allotropic form.In a first stage one-third of the H_2S is oxidised producing H_2S and SO_2 in a 2:1 ratio. Due to thermodynamics restrictions conversion is limited to 70% at this stage and three to four catalytic stages are needed to obtain 95–98% conversion.

The most widely used Claus catalyst in sulphur recovery units is non-promoted spherical activated alumina. These catalysts allow H_2S and SO_2 conversion to elemental sulphur. In addition, they are capable of converting the more stable COS and CS_2, present in low concentration with high efficiency.

$$COS + H_2O \rightarrow H_2S + CO_2$$

$$CS_2 + 2H_2O \rightarrow 2H_2S + CO_2$$

Usually the hydrolysis reactions are verified at the first reactor and an outlet temperature in excess of 360 °C assures its completion.

Alumina catalyst has a key role in optimum sulphur recovery so a deep understanding of its properties is needed. In the present paper alumina catalyst behaviour is studied by means of a Claus reactor model and taking account of alumina fractal properties. Relevant information, about catalyst performance to the Claus reaction is obtained as well as reactor design implications.

2. Fractal dimension

Fractal objects are self-similar structures where increasing magnifications reveal similar features at different length scales [1,2]. Characterisation and analysis of porous objects in terms of fractal geometry has become an intensive research area in recent years. Aggregation and growth phenomena far from equilibrium typically lead to fractal structures. Since during the manufacture process the alumina structure originates from the polymerisation of aluminium hydroxides were aggregates are formed quickly far from

* Present address: CEPSA Technology Department, Madrid, Spain. Tel. +34-922-602710; fax: +34-922-218803.
E-mail addresses: rafael.larraz@tenerife.cepsa.es, rafael.larraz@madrid.cepsa.es (R. Larraz).

1385-8947/02/$ – see front matter
PII: S1385-8947(01)00189-9

Nomenclature

C_c	reactant concentration (units as a function of rate equation)
C_p	specific heat, kJ/kmol °C
d	catalyst diameter (cm)
dv	pore volume differential
D	combined diffusivity (cm^2/s)
D_A	bulk diffusivity (cm^2/s)
D_c	parameter in Eq. (22)
D_{eff}	effective diffusivity (cm^2/s)
D_F	fractal dimension
D_k	Knudsen diffusivity (cm^2/s)
F_i	molar flow (kmol/h)
G	superficial mass flow rate (kg/m^2 h)
$-\Delta H_r$	heat of reaction
M_m	molecular weight
N	number of adsorbed layers
p_0	Fjord escape probability
p_{H_2S}	H_2S partial pressure (atm)
p_{H_2Seq}	H_2S equilibrium partial pressure (atm)
P	total pressure (atm)
P_0	saturation pressure
r	catalyst radius (cm)
r_i	catalyst surface reaction rate
r'	average reaction rate
$r_{macro\ or\ micro}$	macro- or micropore radius (Å)
S	surface area (m^2/g)
T	temperature (K or °C)
V	volume of gas adsorbed
V_1	molar volume (cm^3/mol)
V_m	volume of gas adsorbed in a monolayer
$V_{macro\ or\ micro}$	macro- or micropore volume (cm^3/g)
z	axial coordinate in the reactor

Greek letters

α	parameter in Eq. (19)
β	parameter in Eq. (19)
δ	molecule effective diameter
δ'	δ/δ_{max}
$\delta_{min,\ max}$	minimun, maximun cut-off
Δ	Difference between sulphur low point α reactor outlet temperature, °C
ε	porosity
ϕ	Thiele modulus
Φ	modified Thiele modulus
γ	surface tension (dyn/cm), parameter in Eq. (22)
η	effectiveness factor
$\rho_{s\ or\ p}$	solid or pellet density
ρ_B	bed density
σ	Lennard–Jones constants
Ψ_0	factor as defined in Eq. (9)
Ω	collision integral, unity if molecules are considered rigid spheres
Ω_R	reactor cross-area (m^2)

equilibrium, internal surface of alumina has been suspected as fractal on molecular scales. This fact has been confirmed experimentally [3]. Coppens and Froment have applied fractal structure of Pt-Re-alumina catalyst to the catalytic naphtha reforming process finding influence of fractal dimension over the process conversion and product selectivity [4].

Fractals has been described as objects able to simulate diffusion controlled process structures as catalyst [5]. Avnir et al. made an important observation from the analysis of many adsorption data published in the literature: for a large number of porous media, including many catalyst, the measured surface area S depends on the effective diameter δ of the sorbate molecules according to simple power law

$$S \approx \delta^{-a} \tag{1}$$

The so-called fractal dimension D_F, expresses the space filling capacity of a fractal. While Euclidean shapes have integer dimensions (1 for a line, 2 for a surface and 3 for a volume), a catalyst surface can have any dimension between 2 and 3, both limits included. Many fractals in nature can be very well approximated by a statistical self-similar or self-affine structure. A real object can only be self-similar, fractal, within a finite fractal scaling range, the inner and outer cut-offs, δ_{min} and δ_{max}. Informally the number N of units of size δ needed to cover a fractal object decreases with δ as

$$N \approx \delta^{-D_F} \tag{2}$$

Lengths are measured as $N\delta$, areas as $N\delta^2$, so that in Eq. (1), $a = 2 - D_F$ and becomes

$$S \approx \delta^{2-D_F} \tag{3}$$

Several methods for fractal dimension determination has been described using the information of the complete adsorption isotherm of a single probe [6,7]. Small angle X-ray scattering (SAXS) can be also used to study the mass fractal and surface morphology of materials [8–10].

3. Claus reactor model

In Claus process plants, wide but shallow beds are used. The beds are adiabatic with the possible exception of the region adjacent to the insulated vessel walls. In the absence of localised channelling, radial temperature and concentration gradients are thus minimised. It may be reasonably expected that a adiabatic one-dimensional reactor model should suffice in simulating Claus converters. The model is described by the following equations:

$$\frac{dF_{H_2S}}{dz} = \rho_B \Omega_R r'_{H_2S} \tag{4}$$

$$\frac{dT}{dz} = \frac{\rho_B M_m}{(Gc_p)\sum(-\Delta H_f^0) r'_{H_2S}}, \qquad r'_{H_2S} = \eta r_{H_2S} \tag{5}$$

with initial conditions $F = F_0$, $T = T_0$ at $z = 0$.

The temperature and production rates are obtained, for each dz, from

$$T = T + \mathrm{d}T, \qquad F_{\mathrm{H_2S}} = F_{(\mathrm{H_2S})} - \mathrm{d}F_{\mathrm{H_2S}},$$
$$F_{\mathrm{SO_2}} = F_{(\mathrm{SO_2})} - 0.5\,\mathrm{d}F_{\mathrm{H_2S}}, \quad F_{\mathrm{S}_x} = F_{\mathrm{S}_x} + (\tfrac{3}{2}x)\mathrm{d}F_{\mathrm{H_2S}},$$
$$x = 2, 3, 4, 5, 6, 7, 8, \qquad F_{\mathrm{H_2O}} = F_{(\mathrm{H_2O})} + \mathrm{d}F_{\mathrm{H_2S}} \qquad (6)$$

where S_6 and S_8 are the main sulphur allotropic forms at reactor operating conditions. Claus reaction is considered as a moderate exothermic reversible reaction coupled with sulphur allotropic thermodynamic transformation reactions. These reactions are considered fast so sulphur allotrope equilibrium composition is achieved. Fourth-order Runge–Kutta numerical integration scheme for solving ordinary differential equations was employed to integrate the equations through the fixed bed reactor. Particularities of effectiveness factor calculation and reaction rate expression for the Claus reaction are described below.

4. Claus reaction effectiveness factor

Catalysts are highly porous materials, and typically show some aspects of pore diffusion control. The effectiveness factor, η, for a catalyst is defined as the ratio of the average reaction rate, r', divided by the rate at catalyst's surface, r. When the reaction rate presents constraints due to the porous structure of the catalyst pellet, the true reaction rate is given by

$$\mathrm{r}' = \eta r \quad \text{and} \quad \eta = f(\phi) \qquad (7)$$

where ϕ, the Thiele modulus, is the ratio of the reaction rate to the diffusion rate and is given by [11]

$$\phi = \frac{1}{3} r \left(\frac{r \rho_{\mathrm{p}}}{D_{\mathrm{e}} C_{\mathrm{c}}} \right)^{1/2} \qquad (8)$$

Effectiveness factor includes various potential rate-controlling factors such as the intrinsic catalytic reaction rate, both inter- and intra-particle mass and heat transfer rates, and the physical properties of the catalyst particles.

Effectiveness factor calculation for Claus reaction involves considerable complexity due to the presence of multiple reaction steps in the system and the reversibility of the Claus reaction. The calculation of a local isothermal effectiveness factor depends upon the feed composition to the reactor, the extent of the conversion and the temperature at the exterior of the catalyst particle. Razzaghi and Dalla Lana [12] have proposed the use of a modified Thiele modulus, Φ, and a η–Φ curve applicable for the Claus reaction in the 500–600 K operating temperature range. The modified Thiele modulus has the form

$$\Phi = \frac{\phi}{\sqrt{(1 - \Psi_0)}} \qquad (9)$$

where $\Psi_0 = p_{\mathrm{H_2Seq}} / p_{\mathrm{H_2S}}$ is included due to the thermodynamic equilibrium restriction inherent to the Claus reaction.

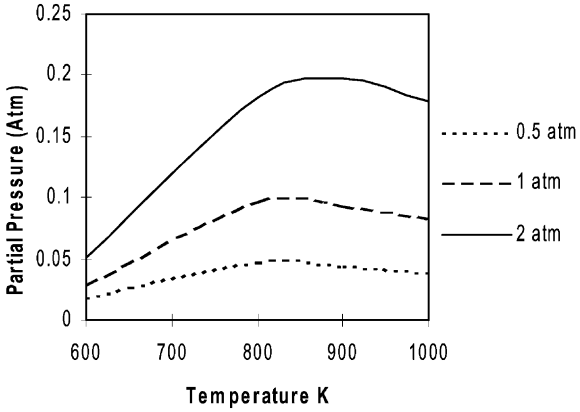

Fig. 1. H_2S equilibrium partial pressure.

The H_2S equilibrium partial pressure is calculated through the Gamson and Elkins [13] procedure the calculations results are shown in Fig. 1. The η–Φ curve is presented in Fig. 2.

Effectiveness factor evaluates the pore structure influence in the catalyst performance. Values close to 1, indicates a rapid accessibility of the reactants to the active sites and products exit from the catalyst, low effectiveness factor means a small catalyst efficiency and poor performance.

In calculating effectiveness factors for the Claus reaction system, the correct intrinsic rate function should be used. Table 1 lists several rate expressions and their authors. The similarity in form between equations independently obtained for different alumina-based catalyst suggests that the catalyst mechanism may be relatively insensitive to the physical structure of the alumina surface. Alternatively, this insensitivity to the catalyst surface could be a consequence of the presence of large amounts of sulphur being adsorbed on the surface, as many authors believe [14,15]. According to Dalla Lana et al. [16] during the reactor calculation procedure a ratio, where the actual area of the catalyst is related to the area in fresh conditions, is included into the rate expression to account for catalyst deactivation due to surface decrease. Reversible deactivation mechanism, as sulphur condensation and alumina sulphation are not considered here. The

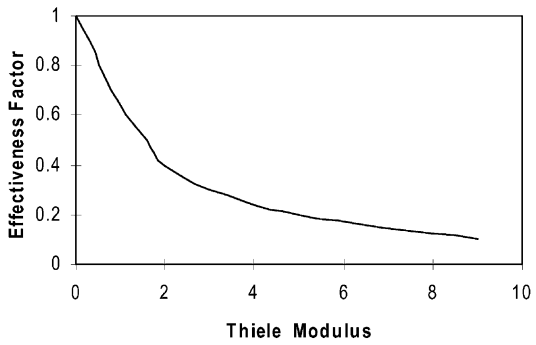

Fig. 2. The η–Φ curve.

Table 1
Intrinsic rate expressions for Claus reaction[a]

Author	Catalyst	k_0	E (J/mol)	b	N
Dalla Lana et al. [16]	Bauxite	6.4E−3	31149	0.0317	1
Dalla Lana et al. [26][b]	Alumina	5.24E−3	30773	0.045	2
George [24][c]	Co-Mo alumina	–	23500	–	1
Quet et al. [23]	Alumina	–	27100	–	1
El Masry [25]	Alumina	–	35100	0	–

[a] $r_{H_2S} = k_0 \exp(-E/RT) p_{H_2S} p_{SO_2}^{0.5}/(1 + bp_{H_2O})^N$.
[b] Equation for reactor calculation.
[c] Low activation energy due to diffusional limitations.

main catalyst deactivation mechanism is due to small pore collapse caused by the water effect over alumina at reactor temperature or by temperature excursions.

5. Random pore model

The pore structure of a catalyst pellet can be conveniently characterised by its pore size distribution determined by porosimetry. For bimodal pore structures, the relevant quantities are

$$V_{\text{marco}} : \text{marcopore volume}, \quad V_{\text{micro}} : \text{micropore volume},$$
$$r_{\text{macro}} = (1/V)_{\text{macro}} \int r \, \mathrm{d}v : \text{macropore average radius},$$
$$r_{\text{micro}} = (1/V)_{\text{micro}} \int r \, \mathrm{d}v : \text{microproe average radius},$$
$$\rho_s : \text{solid density} \tag{10}$$

Under the term micropores we are considering pores smaller than 100 Å, macropores are those over 100 Å. Micro- and macropore average radius and volume are obtained by means of nitrogen adsorption and Hg porosimetry. The following properties can be derived from these

$$\rho_p = \frac{1}{(1/\rho_s) + V_{\text{macro}} + V_{\text{micro}}} \tag{11}$$

where ρ_p is the pellet density.

$$\varepsilon_{\text{macro}} = V_{\text{macro}} \rho_p \tag{12}$$

where $\varepsilon_{\text{macro}}$ is the macroporosity.

$$\varepsilon_{\text{micro}} = V_{\text{micro}} \rho_p \tag{13}$$

where $\varepsilon_{\text{micro}}$ is the microporosity.

The surface area of the catalyst is directly related to its pore structure. For bimodal pore structures, as alumina, integral properties allow a reasonably good correlation

$$S = \frac{2V_{\text{macro}}}{r_{\text{macro}}} + \frac{2V_{\text{micro}}}{r_{\text{micro}}} \tag{14}$$

Beyond the surface area, the pore structure also determines the diffusive characteristics of the support. We employ the random pore model of Wakao and Smith [17] in these calculations, since matches very well alumina diffusivity measurements. The random pore model considers both Knudsen diffusion (very small pores) and bulk diffusion (very large pores) and accounts for the transition region. The following equations will be needed for the random pore model

$$D_A = \underbrace{\frac{0.001853 T^{3/2} ((1/M_A) + (1/M_B))^{1/2}}{P_t \sigma_{AB} \Omega_{AB}}}_{\text{bulk difussivity}}, \tag{15}$$

$$D_{k,\text{macro or micro}} = \underbrace{9.7 \times 10^3 r_{\text{macro micro}} \left(\frac{T}{M_A}\right)^{1/2}}_{\text{Knudsen diffusivity}}, \tag{16}$$

$$\frac{1}{D_{\text{macro or micro}}} = \underbrace{\left(\frac{1}{D_A} + \frac{1}{D_{k,\text{macro or micro}}}\right)}_{\text{combined diffusivity}}, \tag{17}$$

With all these, the effective diffusivities are computed from

$$D_{\text{eff}} = \frac{D_{\text{macro}} \varepsilon_{\text{macro}}^2 + \varepsilon_{\text{macro}}^2 (1 + 3\varepsilon_{\text{macro}}) D_{\text{micro}}}{1 - \varepsilon_{\text{macro}}} \tag{18}$$

It is clear that fractal morphology of the surface influences the Knudsen diffusivity of gases, since a molecule with an effective diameter δ can only enter pores larger than δ. An expression has been derived [4,18] for the ratio of the Knudsen diffusivity in a general porous medium with a statistically self-similar internal surface, D_k, and the Knudsen diffusivity in a medium with the same pore network structure, but with a smooth internal surface, D_{k_0}. Hence, the fractal nature of the surface was treated as a perturbation. The ratio D_k/D_{k_0} depends on the smallest accessible indentation or fjord width and is proportional to the effective diameter of the molecule.

According to the work of Coppens [18]. The expression for the Knudsen diffusivity in a porous medium is not a real power law of the effective molecular diameter, and contains besides the fractal dimension, D_F, also an additional parameter, p_0, the probability of escaping out of a fjord where has previously entered, return probability

$$\frac{D_k(\delta')}{D_{k_0}} = \frac{1}{(1 + \alpha(1 - (\delta')^\beta)} \tag{19}$$

with $\delta' = \delta/\delta_{max}$. The coefficients α and β are given by

$$\alpha = \frac{(2 - D_c)(1 + (1/p_0))f}{1 + (2 - D_c)(1 - (1/p_0))} \quad (20)$$

$$\beta = 1 + (2 - D_c)\left(1 - \frac{1}{p_0}\right) \quad (21)$$

with $f = 0.5$, and

$$D_c = \frac{2\log\gamma}{\log(1+\gamma)} \quad \text{and} \quad D_F = \frac{2\log((1/p_0) + \gamma)}{\log(1+\gamma)} \quad (22)$$

These equations are solved for D_k according to the restrictions: D_c should be between 1 and 2, γ should be larger than 1.618 and p_0 should be smaller than $(1.618^{D_F} - 1.618)^{-1}$.

For an explanation about Knudsen diffusivity analytical expression derivation and meaning see [10]. For not too low values of p_0 and δ', the following first order approximation is useful

$$\frac{D_k(\delta')}{D_{k_0}} = (\delta')^{D_F - 2} \quad (23)$$

This equation expresses that the Knudsen diffusivity is inversely proportional to the non-accessible surface area.

6. Alumina fractal dimension calculation

Typical Claus alumina characteristics are presented in Tables 2 and 3. In this work, three alumina catalyst has been considered, their main structural properties, obtained by nitrogen adsorption porosimetry, are shown in Table 4. A1 catalyst is a fresh Claus catalyst with a different micro-, mesopore distribution as can be seen in Fig. 3, where pore size distribution is represented for all the samples. Remaining samples are A1 catalyst at different stages of deactivation after service in an industrial Claus unit. Sample A2 presents mid run stage with a significant decrease of the surface area and modification of the original pore size distribution. Sample A3 has been taken from a heavily deactivated reactor and presents a very low surface area and microporosity as expected in a spent catalyst.

Table 2
Catalytic converters effectiveness factor[a]

Parameter	Reactor 1	Reactor 2	Reactor 3
Temperature (°C)	320	230	215
H_2S (vol.%)	7.5	2	1
H_2O (vol.%)	–	28	39
GHSV (h^{-1})	500	500	500
η	0.14	0.12	0.31

[a] Atmospheric operating pressure.

Table 3
Alumina physical properties

Parameter	Alumina
ρ_s (g/cm^3)	3.15
ρ_p (g/cm^3)	1.24
V_{macro} (cm^3/g)	0.085
V_{micro} (cm^3/g)	0.404
r_{macro} (Å)	5226
r_{micro} (Å)	25
ε_M	0.14
ε_m	0.56
S (m^2)	325
d (cm)	0.6

Table 4

Parameter	A1	A2	A3
BET plot intercept	0.0002	0.00028	0.00184
BET plot slope	0.01303	0.03097	0.1403
r_{micro} (Å)	26	52	91
S (m^2)	328.5	139.1	30.6
$V_{pore} > 10$ Å (cm^3/g)	0.3619	0.325	0.168
$V_{pore} < 45$ Å (cm^3/g)	0.318	0.234	0.037
d (cm)	0.6	0.6	0.6

Fig. 4 shows adsorption–desorption nitrogen isotherm for the alumina samples studied where adsorbed amount V_{ad}, expressed in cm^3 at STP, is plotted as a function of relative vapor pressure P/P_0. The isotherms exhibit an extended hysteresis loop for all the samples, which is a signature of capillary condensation. A progressive diminution of the nitrogen adsorbed and the hysteresis loop size is found as the catalyst deactivates. For the adsorption–desorption isotherm the standard BET analysis were performed and results are given in Table 4.

Fractal analysis found in literature ([19] and references therein) for nitrogen porosimetry are based on fitting adsorption data to an expression relating nitrogen adsorbed to the relative pressure applied. The volume of the adsorbed film is

$$V \propto r^{3-D_F}$$

Typically a linear fit of the adsorption data on a log–log scale is used to find the slope, from which the fractal dimension D_F is obtained. Following such procedure, a plot of $\log(V_{ad}/V_{full})$ versus $\log(r)$ was made, where r was calculated using the well known Kelvin equation

$$r = \frac{2\gamma V_1}{RT\ln(P_0/P)} \quad (24)$$

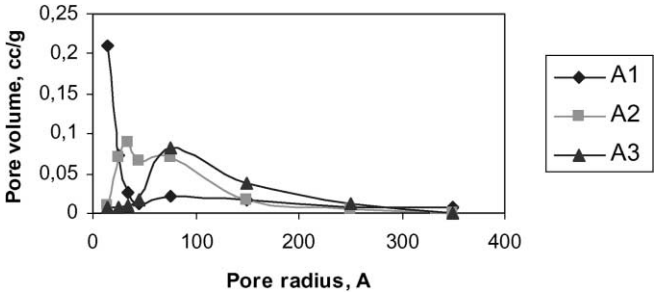

Fig. 3. Alumina samples pore distribution.

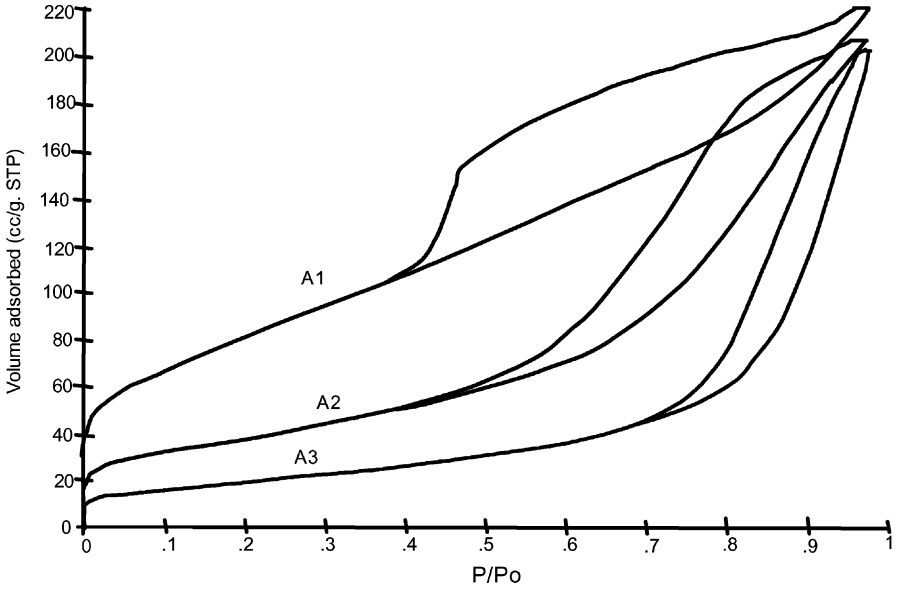

Fig. 4. Alumina adsorption–desorption nitrogen isotherms.

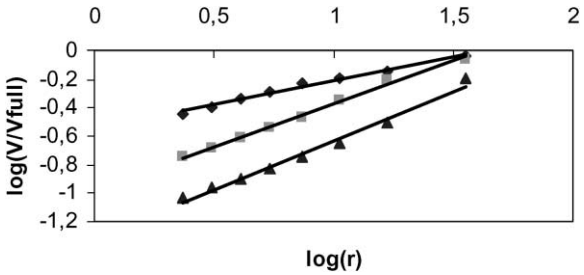

Fig. 5. D_F estimation for A1, A2 and A3 samples; Ma method.

and V_{full} is the volume of nitrogen measured at the maximum p/p_0. The nitrogen adsorption branch data were taken in each sample, due to the fact that during nitrogen desorption pores in the interior part of the catalyst cannot empty until enough pores on the outer part are emptied to make them exposed to the surrounding vapour. The adsorption branch of the isotherm does not suffer from this accessibility problem. Results obtained are shown in Fig. 5 where data correlation to a straight line is confirmed for the samples studied. Fractal dimensions derived from this procedure are presented in Table 5.

Another fractal dimension value estimation method [7,20] has been also used. The method is based in an expression for

Table 5

Parameter	A1	A2	A3
D_F (cm) [19]	2.66	2.40	2.30
r^2	0.98	0.99	0.99
D_F (cm) [20]	2.68	2.39	2.30
r^2	0.98	0.99	0.99
Cut-off range (Å)	3–35	3–35	3–35

the surface fractal dimension from an analysis of multilayer adsorption to a fractal such that

$$\ln\left(\frac{V}{V_m}\right) = C + S\ln\left(\ln\left(\frac{P_0}{P}\right)\right) \quad (25)$$

where V is the volume of gas adsorbed at an equilibrium pressure, P, V_m the volume of gas in a monolayer, and P_0 is the saturation pressure. The constant C is a pre-exponential factor and S is a power law exponent dependent on D_F, the surface fractal dimension, and the mechanism of adsorption. There are two limiting cases: at the lower end of the isotherm, representing the early stages of multilayer build-up, the film/gas interface is controlled by the attractive van der Waals forces between the gas and solid which tends to make the film/gas interface replicate the surface roughness. In this case the value of the constant S is given by

$$S = \tfrac{1}{3}(D_F - 3) \quad (26)$$

At higher coverage the interface is controlled by the liquid/gas surface tension which makes the interface move further away from the surface so as to reduce the interface area. In this second case S is given by

$$S = D_F - 3 \quad (27)$$

Under both circumstances the ratio V/V_m is related to the number of adsorbed layers, N, by

$$N = \left(\frac{V}{V_m}\right)^{1/(3-D_F)} \quad (28)$$

The actual thickness of coverage is obtained multiplying by the diameter of the adsorbate molecule (3.5 Å for nitrogen). The length-scale cut-offs encompassed by the surface fractal dimension is the thickness of the adsorbed multilayers over which the fractal dimension applies.

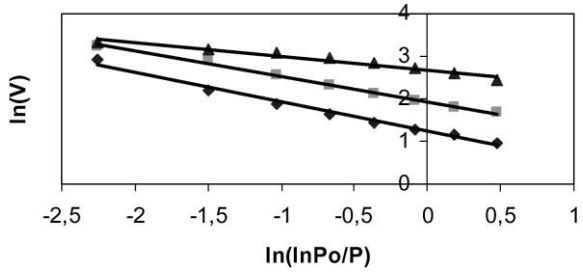

Fig. 6. D_F estimation for A1, A2 and A3 samples; Pfeifer method.

Fractal dimension of these samples as well as cut-off values has been calculated according to the described procedure. Results obtained are presented in Table 5 and Fig. 6 also including correlation factor and cut-off range where fit to Eq. (25) is linear. Eq. (27) provides unrealistic fractal dimension values so Eq. (26) was employed.

Both fractal dimension calculation procedures gives similar values for the three samples. Results obtained points to the fact that Claus catalyst presents a fractal dimension of 2.67. As catalyst deactivation proceeds, catalyst fractal dimension diminishes. Mid age catalyst A2 has a fractal dimension of 2.40. Severe deactivated catalyst presents a 2.30 fractal dimension. Deactivated samples microporosity is smaller than fresh catalyst and mean pore radius increases from 26 to 52 and 91 Å, respectively, fractal character seems to be related to the smaller pores those that keeps the main part of the catalyst surface area.

Catalyst cut-offs from the samples analysed remains into the 3–35 Å pore radius range so fractal structure is restricted to Claus catalyst micro- and mesoporosity. Although pores smaller of 7.5 Å has no catalytic activity due to the size of the sulphur molecule, the 7.5–35 Å range still represent a big part of the catalyst active surface area. Fig. 7 presents the maximum pore diameter that plugs with liquid sulphur as a function of the reactor temperature and the difference between sulphur dew-point and the reactor temperature [21].

From the figure it can be inferred that if reactor temperature is 5 °C higher than dew-point, pores with diameters greater than 23 Å (11.5 Å pore radius) are still free of sulphur condensation. An estimation of fractal dimension in the range of 11–35 Å gives values of 2.70, 2.39 and 2.27 for the A1, A2 and A3 samples, respectively. In general Claus plant operators maintain dew-point margins around 8–10 °C [22] so fractal dimension is able to characterise the catalyst surface area at industrial operating conditions.

7. Model results and discussion

Claus reactor performance has been obtained by means of reactor modelling for different alumina catalysts taking account of its fractal structure. Intrinsic rate expressions for the Claus reaction taken from the bibliography are shown in Table 1, second expression was the rate expression employed in the modified effectiveness factor analysis [12] and has been the one employed into the reactor calculation. Operating conditions of reactor stages at a Claus unit are described in Table 2. Third stage conditions has been employed in the simulations where low reactor concentrations and high water content constraints reactants conversion.

The reactor simulation procedure calculates effectiveness factor for the Claus reaction over alumina catalyst depending on alumina pore structure parameters. Initial data consists of reactor operating conditions and catalyst structural properties as shown in Tables 2–4. Knudsen diffusivity accounting for the catalyst fractal dimension is employed for the micropores; calculation sequence is presented in Fig. 8. This modified expression of the Knudsen diffusivity, D_k, is used in the effectiveness factor calculation and provides a different value for the effectiveness factor of the Claus reaction. Although a small maximum exists for extreme values of p_0, in general if we consider the fractal nature of alumina, lower effectiveness factor than smooth surface catalyst are obtained as fractal dimension increases. Operating conditions

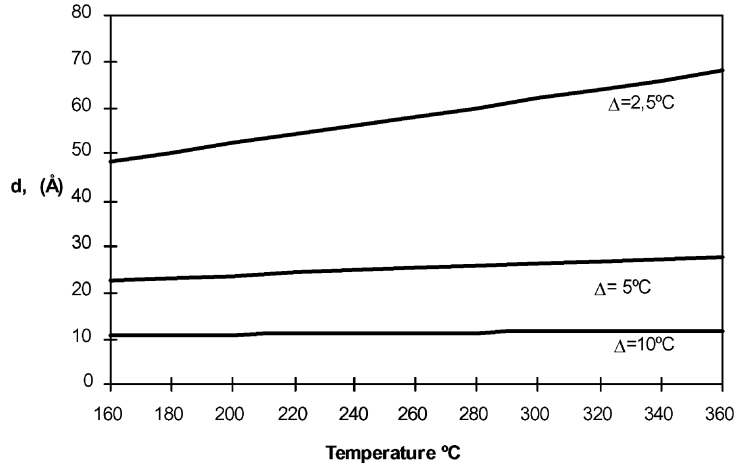

Fig. 7. Reactor temperature influence over pore plugging due to sulphur condensation as a function of dew-point and reactor temperature.

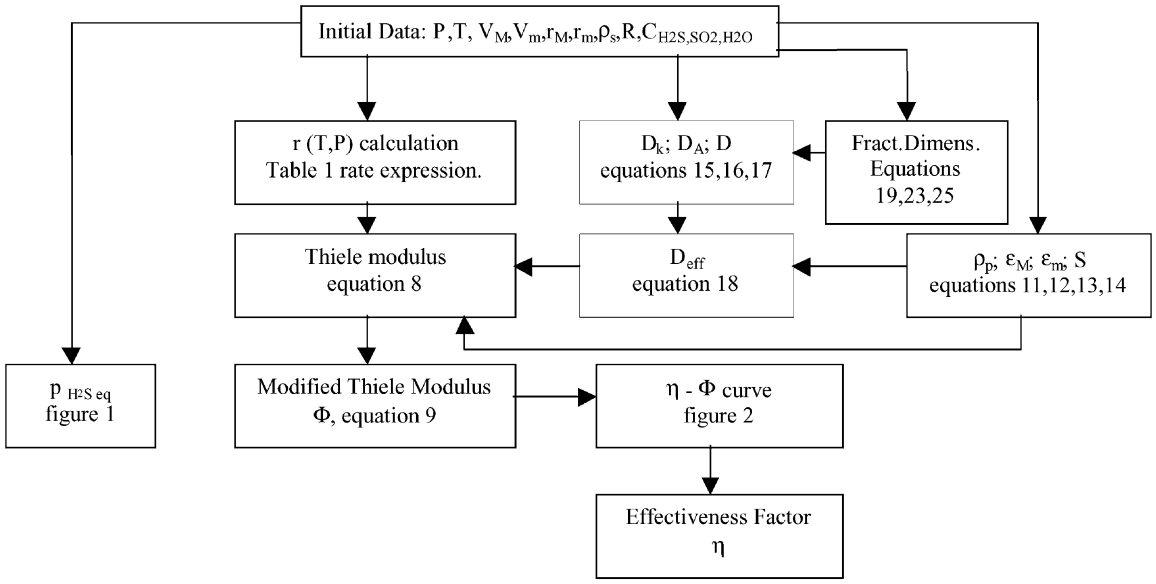

Fig. 8. Effectiveness factor calculation procedure.

reproduces industrial plant third reactor. Water content of reactor feed thermodynamically constraint H_2S conversion to values below 90%. Reactor temperature rise varies between 15 °C for the fresh catalyst and 4 °C for the spent A3 sample.

Fractal dimension effect over reactor performance is presented in Fig. 9a and b where fractal dimension is varied from 2 to 3 at 0.2 intervals and the reactor conversion (%) expressed as

$$\text{conversion} = \frac{H_2S_{inlet} - H_2S_{outlet}}{H_2S_{inlet}}$$

as well as effectiveness factor are included. Firstly Eq. (19) was employed for the D_k estimation. Up to $D_F = 2.6$ a H_2S conversion decrease from 0.827 to 0.773 is obtained as the fractal dimension increases. Effectiveness factor diminishes with fractal dimension from 0.33 to 0.22. For fractal dimensions higher than 2.6 a slight increase of conversion and effectiveness factor is observed, Fig. 9a, at $D_F = 3$ conversion and effectiveness reach 0.812 and 0.286, respectively. This fact has been predicted by Coppens [10] and is related to the return probability, p_0, value at high fractal dimensions. When Eq. (23) is used for D_k estimation, conversion and effectiveness values decreases monotonically with the fractal dimension as can be seen in Fig. 9b.

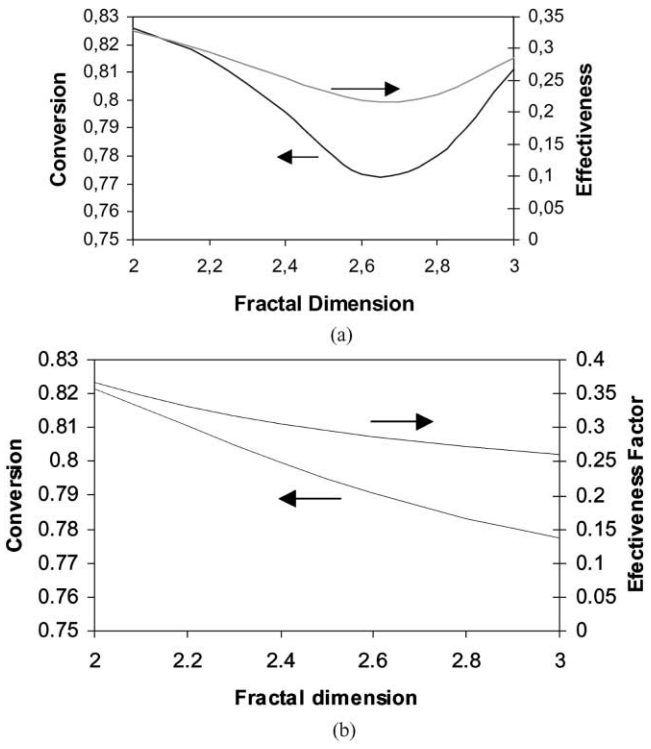

Fig. 9. (a) Fractal dimension influence over H_2S conversion and effectiveness factor (Eq. (19)); (b) Fractal dimension influence over H_2S conversion and effectiveness factor (Eq. (23)).

Model results are presented in Fig. 10, H_2S conversion along the reactor is presented for the A1, A2 and A3 smooth and fractal catalyst where fractal dimension is estimated over the 3–35 Å cut-off range. Smooth catalyst, those with fractal dimension $D_F = 2$, shows the best behaviour performing an approximately 5–6% higher conversion than fractal ones at reactor outlet for the A1 and A2 samples. For A3 deactivated catalyst this difference is lower and less than 1%. The spent catalyst presents an indiscernible behaviour between the smooth and fractal catalyst due to the low value of the fractal dimension, 2.30, and the low reaction rates at these conditions.

Effectiveness factor and Knudsen diffusivity are presented in Table 6. The minimum effectiveness factor and Knudsen diffusion values are obtained for the fractal A1 sample, 0.214 and 2.3×10^{-7} cm^2/s, respectively.

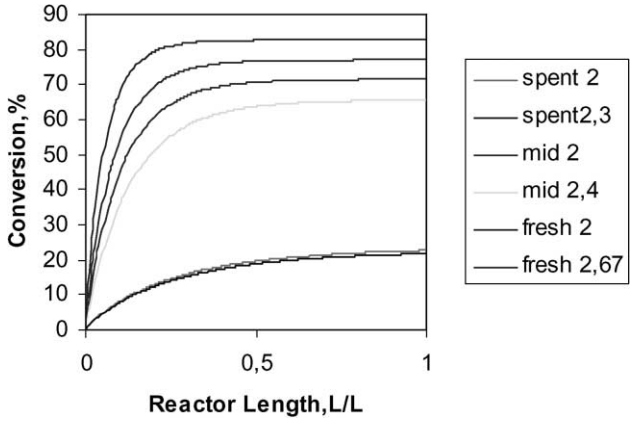

Fig. 10. Fractal and smooth alumina catalyst performance, 3–35 Å cut-off range.

Table 6

Parameter	Smooth	A1	A2	A3
D_k (cm^2/s)	0.009	2.3×10^{-7}	0.005	0.014
η	0.327	0.214	0.284	0.290
D_F (cm)	2	2.68	2.39	2.30

Regarding conversion evolution through the reactor bed, using the smooth catalyst a 0.75 conversion value is obtained at 14.2% of reactor length whilst the fractal catalyst needs a 32.6% of reactor length to obtain the same conversion. For design purposes the catalyst fractal structure should involve higher reactor volumes than expected for the smooth one.

8. Conclusions

Claus catalyst reactor performance has been studied taking account of its fractal porous structure described by the fractal dimension parameter. Fractal dimension has been calculated employing methods based on nitrogen adsorption porosimetry. A reactor model has been used that considers a modified effectiveness factor, which includes Claus reaction characteristics.

The analysed Claus catalyst samples presents fractal dimensions in the 2.67–2.30 range, restricted to micropores among 3–35 Å pore radius. Fractal dimension significantly modifies reactor performance increasing reactor volume needed to obtain the same H_2S conversion. Fractal dimension decreases as catalyst deactivates presenting a 2.30 value for severe deactivated samples. Influence of fractal dimension over deactivated catalyst is low. Only irreversible deactivation mechanism as surface area loss due to pore blockage, thermal and hydrothermal aging has been considered in this work. Similarity of fractal dimensions obtained in the 11–35 Å range, which is representative of Claus catalyst accessible porosity at industrial operation conditions, and in the 3–35 Å range extends applicability of fractal paradigm to the Claus reaction.

In spite of further experimentation is needed in order to confirm these results, fractal character of the Claus alumina catalyst appears as an important factor in the performance of Claus units and fractal dimension estimation could help during the catalyst selection procedure.

Acknowledgements

The author wishes to express his thank to the referees for their valuable comments and to Prof. Jose Victor Rios from Pennsylvania University for some fruitful discussions about the fractal dimension concept.

References

[1] B. Mandelbrot, The Fractal Geometry of Nature, Tusquet, Barcelona, 1997.
[2] D. Avnir, D. Farin, P. Pfeifer, J. Chem. Phys. 79 (1983) 3566–3571.
[3] D. Avnir, The Fractal Approach to Heterogeneous Chemistry, Wiley, Chichester, 1989.
[4] M.O. Coppens, G.F. Froment, Chem. Eng. Sci. 50 (1995) 1013–1026.
[5] D. Avnir, D. Farin, P. Pfeifer, Nature 308 (1984) 261–263.
[6] A. Neimark, Physica A 191 (1992) 258–262.
[7] P. Pfeifer, D. Avnir, D. Farin, Nature 308 (1984) 261.
[8] A. Guinier, G. Fournet, C.L. Walker, K.L. Yudowitch, Small Angle Scattering of X-rays, Wiley, New York, 1955.
[9] P.W. Schmidt, J. Appl. Cryst. 24 (1991) 414.
[10] M.O. Coppens, Catal. Today 53 (1999) 225–243.
[11] P.B. Weisz, J.S. Hicks, Chem. Eng. Sci. 17 (1962) 265.
[12] M. Razzaghi, I.G. Dalla Lana, Can. J. Chem. Eng. 62 (1984) 413–418.
[13] B.W. Gamson, R.H. Elkins, Chem. Eng. Prog. 49 (4) (1953) 203–215.
[14] M. Steinjs, P. Mars, Ind. Chem. Prod. Res. Dev. 16 (1) (1977) 35–41.
[15] S. Mendioroz, V. Muñoz, E. Alvarez, J.M. Palacios, Appl. Catal. Gen. 132 (1995) 111–126.
[16] I.G. Dalla Lana, D.E. McGregor, C.L. Liu, E. Cormode, in: Proceedings of the 4th Europe/2nd International Symposium on Chem. Eng. Reac. Eng., Elsevier, Amsterdam, 1972, pp. 9–18.
[17] N. Wakao, J.M. Smith, Chem. Eng. Sci. 17 (1962) 825.
[18] M.O. Coppens, Fractals in Engineering, Springer, Berlin, 1997, pp. 336–349.
[19] J. Ma, H. Qi, P. Wong, Phys. Rev. E 59 (1999) 2049.
[20] S.P. Rigby, Catal. Today 53 (1999) 207–223.
[21] G.R. Schoofs, Hydrocarbon Processing,1985, pp. 71–73.
[22] J.A. Sames, Optimizing Claus Sulphur Plant Operations, Sulphur Recovery Seminar, Estanbul, 1995, pp. 5–17.
[23] C. Quet, J. Tellier, R. Voirin, Catalyst Deactivation, 1980, pp. 323–329.
[24] Z.M. George, J. Catal. 32 (1974) 261–271.
[25] H.A. El Masry, Appl. Catal. 16 (1985) 301–313.
[26] I.G. Dalla Lana, C.L. Liu, B.K. Cho, in: Proceedings of the 4th International Symposium on Chem. React. Eng., Vol. 196–205, Frankfurt, 1976.